Interpretation of High Projections for Global-Mean Warming

T. M. L. Wigley[1]* and S. C. B. Raper[2]

The Intergovernmental Panel on Climate Change (IPCC) has recently released its Third Assessment Report (TAR), in which new projections are given for global-mean warming in the absence of policies to limit climate change. The full warming range over 1990 to 2100, 1.4° to 5.8°C, is substantially higher than the range given previously in the IPCC Second Assessment Report. Here we interpret the new warming range in probabilistic terms, accounting for uncertainties in emissions, the climate sensitivity, the carbon cycle, ocean mixing, and aerosol forcing. We show that the probabilities of warming values at both the high and low ends of the TAR range are very low. In the absence of climate-mitigation policies, the 90% probability interval for 1990 to 2100 warming is 1.7° to 4.9°C.

The Third Assessment Report of the Intergovernmental Panel on Climate Change (*1*) gives new projections for global-mean warming in the absence of policies to limit climate change, based on a new set of emissions scenarios, the SRES scenarios (*2*, *3*). The full warming range over 1990 to 2100, 1.4° to 5.8°C (*4*), obtained by using a simple upwelling-diffusion energy-balance climate model (*5*, *6*) calibrated against the results of seven state-of-the-art coupled atmosphere–ocean general circulation models (AOGCMs) (*4*, *7*), is substantially higher than the range given for the earlier IS92 scenarios in the IPCC Second Assessment Report (SAR), 0.8° to 3.5°C (*8*). This change is largely due to the new emissions scenarios [particularly emissions of sulfur dioxide (SO_2)], the incorporation of climate feedbacks in modeling the carbon cycle (*9*), improved relationships between radiative forcing and greenhouse-gas abundances (*10*), more comprehensive treatments of methane and tropospheric ozone (*11*), the direct use of AOGCM results (*12*), and different assumed rates of slowdown of the ocean's thermohaline circulation (THC) (*4*). As noted by Schneider (*3*), Jones (*13*), and Moss and Schneider (*14*), giving only a range of warming results is potentially misleading unless some guidance is given as to what the range means in probabilistic terms (*15*). The purpose of this paper is to provide such guidance.

A common method used to present results probabilistically is to employ a probability density function (p.d.f.), $p(x)$, where the integral of $p(x)$ between x_1 and x_2 gives the probability of x lying in that range. This is the method we use here. The procedure is as follows: first, identify the main sources of uncertainty; second, represent these uncertain elements as p.d.f.s; third, use selected values from these input p.d.f.s to drive a suitable climate model; and finally, combine the various climate model results into an output p.d.f. In the terminology of Moss and Schneider (*14*), this is a Bayesian type of analysis in that the input p.d.f.s must contain some subjective elements. The transfer from input values to output, however, is deterministic, because our climate model (unlike more complex AOGCMs) translates inputs directly into an output temperature "signal" with no internally generated "noise" component.

Generating p.d.f.s for projected global warming requires knowledge (or at least credible estimates) of the p.d.f.s of many different uncertain quantities or model parameters that may influence future warming rates. We consider a limited subset of these, which we show capture the main contributions to output uncertainty. We do not consider the effect of possible structural uncertainties in our climate model, nor factors that our model cannot capture (such as gas cycle or climate "surprises"—rapid changes arising from nonlinearities in environmental systems). As discussed in (*13*) and (*14*), accounting for these would lead to wider uncertainty limits than given by our results.

Probabilistic inputs. The input parameters that contribute most to uncertainties in the projections of global-mean temperature are as follows: the emissions of the various gases that are directly or indirectly radiatively active; the transfer functions that relate emissions to abundances to forcing; the sensitivity of the climate system to external forcing (i.e., the "climate sensitivity," characterized by the equilibrium global-mean warming for a doubling of the CO_2 level, $\Delta T2\times$); and ocean mixing factors that determine the lags between forcing and response. Previous studies (*4*, *8*, *16*–*19*) have concluded that uncertainties in future emissions and in the climate sensitivity are the most important of these factors. The next most important factor appears to be the carbon cycle (*17*), uncertainties in which have been quantified more rigorously in the TAR than previously (*9*).

Emissions uncertainties, using transfer functions from emissions to abundances to forcing as formulated in the TAR, give a 1990 to 2100 total forcing range of ~3.1 to 8.1 W/m^2. For any given value of the climate sensitivity, this forcing range implies a range of values for 1990 to 2100 warming. Similarly, for any given forcing there is a range of possible warming values due to uncertainties in the climate sensitivity. Both ranges are similar in magnitude (*4*, *8*, *20*). In other words, emissions and sensitivity uncertainties have similar consequences for global-mean temperature. If carbon cycle uncertainties are quantified in terms of radiative forcing, the forcing range across all 35 SRES scenarios is expanded by ~1.9 W/m^2. Although this is much smaller than the 3.1 to 8.1 W/m^2 forcing range that characterizes emissions uncertainties, it is still considerably larger than the uncertainty ranges arising from other sources (*17*, *18*, *21*).

The other sources of uncertainty that we consider here are radiative forcing due to aerosols, particularly sulfate aerosols, and ocean mixing (i.e., the efficiency with which heat is transported from the surface into the deeper ocean). The present-day uncertainty range for aerosol forcing is very large. However, this has only a relatively small effect on future warming for most of the SRES scenarios, mainly because of the 21st-century declines in SO_2 emissions that are typical of these scenarios (*21*, *22*). (This contrasts with the SAR, where large 21st-century increases in SO_2 emissions under the IS92 scenarios led to large aerosol-related uncertainties in global-warming projections.) For ocean mixing, the two determinants in our climate model are the vertical diffusivity and changes in the intensity of the THC. THC changes in our simulations are tied directly to the climate sensitivity (see below) because higher sensitivity AOGCMs have more rapid declines in the THC [(*4*), Appendix 9.1)]. We therefore consider only uncertainties in the vertical diffusivity,

[1]National Center for Atmospheric Research, Boulder, CO 80307, USA. [2]Climatic Research Unit, University of East Anglia, Norwich, NR4 7TJ, UK and Alfred-Wegener-Institut for Polar and Marine Research, D-27515 Bremerhaven, Germany.

*To whom correspondence should be addressed. E-mail: wigley@ucar.edu

which we know a priori have only a minor effect on warming projections (*16*).

We now have five factors for which we must estimate p.d.f.s to drive our climate-model projections. For emissions, the SRES report (*2*) states that "There is no single most likely, 'central,' or 'best-guess' scenario, either with respect to SRES scenarios or to the underlying literature" and does not assign probabilities or likelihoods to individual scenarios [(see also (*3*)]. We therefore assume all 35 emissions scenarios to be equally likely. This leads to a rather uneven distribution of input radiative forcings, as shown in Fig. 1.

For the climate sensitivity, the range of values used in the IPCC TAR temperature projections is 1.7° to 4.2°C (*4*). This is derived from the set of seven AOGCMs upon which the range of future warmings in the TAR is based. These values do not span the full range of possible sensitivities, as is noted in the TAR (*4*). In previous IPCC work, the standard uncertainty range given is 1.5° to 4.5°C, but no confidence interval has been stated. We assume here that 1.5° to 4.5°C corresponds to the 90% confidence interval (*23*). We consider two different p.d.f.s, a uniform distribution and a log-normal distribution (Fig. 2).

To define the log-normal distribution fully, we also prescribe the median sensitivity. In previous IPCC assessments, the best-estimate sensitivity value has been assumed to be 2.5°C, which implies that the distribution is skewed to the left. We assume a slightly less skewed distribution here, using the median sensitivity of the seven TAR AOGCMs (2.6°C) as our median value.

The third uncertainty factor we consider is the carbon cycle. The carbon cycle model we use here is that of Wigley (*24*), as employed in both the TAR (*4*) and SAR (*8*). The model includes both CO_2 fertilization and climate feedbacks. For the TAR, the model's climate feedbacks were tuned to give atmospheric CO_2 abundances for the SRES scenarios that closely matched those for other models (*25*, *26*) used elsewhere in the TAR. In the TAR temperature projections, uncertainties in these feedbacks were not considered. This gave a range of 2100 abundance projections across the SRES scenarios of 540 to 970 parts per million (ppm). The full uncertainty range given in the TAR (*9*), accounting for feedback uncertainties, is 490 to 1260 ppm. To cover this full uncertainty range here, we defined p.d.f.s for the parameters in our carbon cycle model that gave 490 to 1260 ppm as the extreme range over all 35 emissions scenarios. We found that, for any emissions scenario, the output distribution of CO_2 abundances could be well simulated by applying simple linearly time-dependent scaling factors to the central estimate used for the TAR temperature projections. (Time-dependent scaling is necessary because the uncertainty range must increase as time increases.) This allows a considerable simplification in the calculations required to determine the relative importance of carbon-cycle model uncertainties and produces results that are consistent with the uncertainty range estimated in the TAR.

For aerosol forcing (the sum of direct and indirect sulfate, biomass, and carbonaceous aerosols (*4*)], we employed the TAR central estimate (-1.3 W/m^2 in 1990) as the median for a log-normal p.d.f. and chose 5 and 95% limits of -0.3 W/m^2 and -1.9 W/m^2, using uncertainty estimates given in the TAR together with constraints based on fitting our climate model to observed global- and hemispheric-mean temperatures [(compare with (*27*)]. For oceanic vertical diffusivity, we also assumed a log-normal p.d.f. with 5, 50, and 95% values of 1.3, 2.3, and 4.1 cm^2/s, on the basis of results given in the TAR [(*4*), Appendix 9.1]. Because our output temperature p.d.f.s are insensitive to aerosol forcing and diffusivity uncertainties (see below), uncertainties in the above two p.d.f.s are relatively unimportant.

Climate model results. The climate model used here is the same as that used in the TAR (*4*–*6*). Simulations run from 1765 to 2100. The full set of SRES emissions scenarios, together with p.d.f.s that capture carbon cycle and aerosol forcing uncertainties, give a wide range of radiative forcing projections that drive this model (*28*). The model itself requires specific values to be set for a number of different parameters [(*4*), Appendix 9.1)] For climate sensitivity and vertical diffusivity we used p.d.f.s as described above. All other parameters were linearly interpolated as functions of sensitivity, preserving the values that corresponded to the highest and lowest sensitivity cases. This is a useful simplifying procedure that has no noticeable effect on the results presented below,

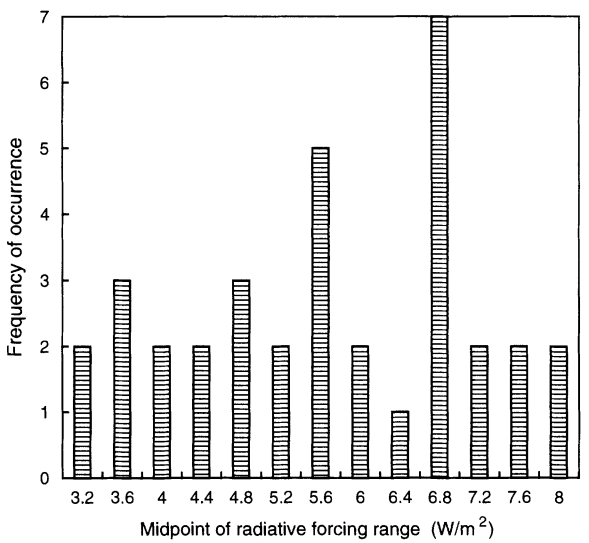

Fig. 1. Frequency of occurrence of different 1990 to 2100 radiative forcing ranges under the SRES emissions scenarios based on TAR relationships between emissions, abundances, and radiative forcings. Because of climate feedbacks on the carbon cycle, the precise forcing for any given scenario depends on the warming, which, in turn, depends on the assumed climate sensitivity. The values here use a sensitivity of $\Delta T2\times = 2.6$°C.

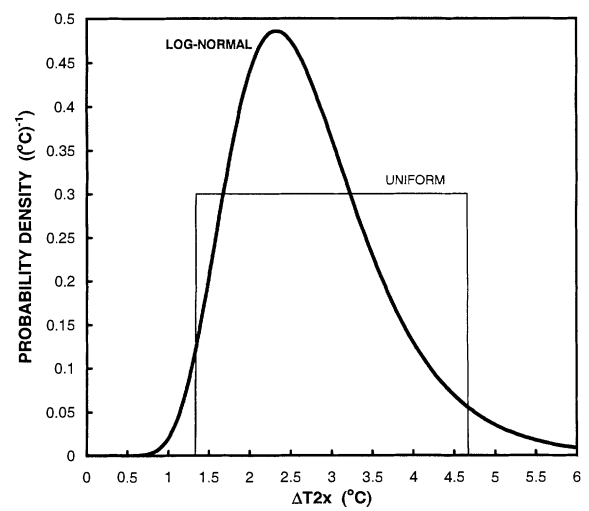

Fig. 2. Distribution functions (probability densities) assumed for the climate sensitivity, expressed as the equilibrium warming for $2\times CO_2$ ($\Delta T2\times$). Both cases have 1.5° to 4.5°C as the 90% probability interval.

primarily because of the dominant influence of the climate sensitivity.

To obtain climate model output results in terms of probability distributions, results for each of the 35 SRES emissions scenarios were given equal weight, and the p.d.f.s for climate sensitivity, CO_2 abundance, aerosol forcing, and oceanic vertical diffusivity were divided into equiprobable fractiles. Temperature projections were then made with parameter values corresponding to the median of each fractile. We used 25 fractiles for climate sensitivity and quintiles for the three other factors (requiring 109,375 climate model simulations for our final results). We refer to this method as Exhaustive Fractile Sampling, because it considers all possible combinations of results for the division of the input distributions into prespecified fractiles. It is similar to the commonly used method of Latin Hypercube Sampling (*29*), in which fractile combinations are chosen by random sampling.

Figure 3 gives the distributions of 1990 to 2100 warming for three cases: (i) all emissions scenarios plus a uniform p.d.f. for climate sensitivity and single (median) values for all other parameters; (ii) as in (i), but using a log-normal p.d.f. for sensitivity; (iii) as in (ii), but including carbon cycle uncertainty effects. The output distributions are very similar, demonstrating that the results are robust to uncertainties in the shape of the input distribution for climate sensitivity, and that the effect of incorporating carbon cycle uncertainties into the assessment is minor. The differences between the three distributions are illustrated in terms of specific percentiles in Table 1. The fact that the log-normal distribution is skewed to the left and has a lower median than the uniform distribution (2.6°C versus 3.0°C) shifts the output temperature distribution slightly to the left relative to the uniform p.d.f. case. When carbon cycle uncertainties are included, the low and (especially) high tails of the distribution are expanded (Fig. 3 and Table 1), and the probability of large warming is increased.

Figure 4 shows how the distribution of warming changes with time for the log-normal sensitivity case with carbon cycle, aerosol forcing, and diffusivity uncertainties included. Comparison with Fig. 3 shows that the addition of aerosol and diffusivity uncertainties has little effect on the results. (The differences are quantified in Table 1.) As expected, the uncertainty range increases with time. Even for changes over 1990 to 2030, there is considerable uncertainty; the 90% probability interval is 0.5° to 1.2°C (for changes over 2000 to 2030, subtract 0.2°C). The median projected warming rate, 0.20°C/decade, is comparable to the warming rate that has occurred over the past 25 years (*30*). By 2100, the 90% probability interval for warming from 1990 has expanded to 1.7° to 4.9°C; and the median warming rate over 1990 to 2100 is 0.28°C/decade. Comparing this interval with the range 1.4° to 5.8°C given in the IPCC TAR shows that warming at the high and low ends of this range is unlikely. Another more salutary comparison is between the median 1990 to 2100 warming rate and the observed warming rate over the past 100 years of ~0.06°C/decade. The projected median warming rate is approximately five times that of the past.

Caveats and conclusions. The results

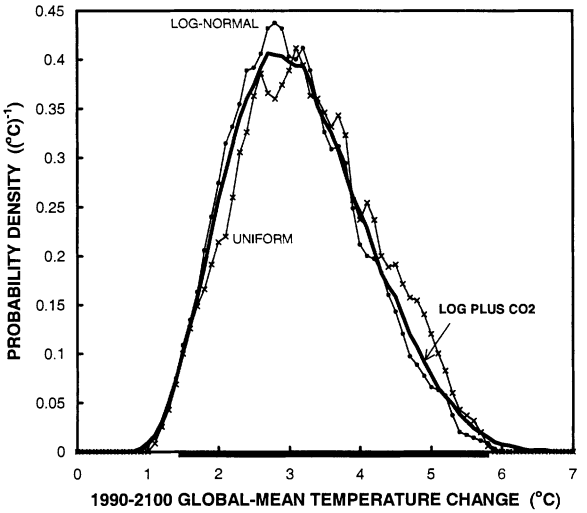

Fig. 3. Sensitivity of the distribution of global-mean warming over 1990 to 2100 to the assumed distribution function for climate sensitivity [compare LOG-NORMAL (dotted line) and UNIFORM (crosses)], and to the inclusion of the effects of carbon cycle uncertainties [compare LOG-NORMAL and LOG PLUS CO_2 (bold line)]. Warming distributions have been smoothed with a 1:2:1 binomial filter. The bar under the temperature axis shows the IPCC TAR range.

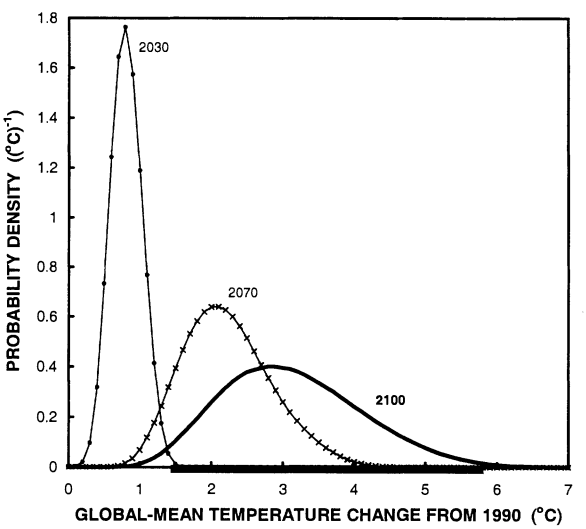

Fig. 4. Evolution of uncertainties in global-mean warming, illustrated by warming distributions over 1990 to 2030 (dotted line), 1990 to 2070 (crosses), and 1990 to 2100 (bold line). This is the log-normal sensitivity case with carbon cycle, ocean mixing, and aerosol forcing uncertainties included. Warming distributions have been smoothed with a 1:2:1 binomial filter. The bar under the temperature axis shows the IPCC TAR 1990 to 2100 warming range. For the 2100 p.d.f., the probability of warming less than 1.4°C is 1.7%, and of warming above 5.8°C is 0.6%. The 2030 result is similar to that of (*40*).

Table 1. Percentile values for global-mean warming (°C) from 1990 to the year indicated. Top two rows: 1990 to 2100 warming for different assumed climate sensitivity distributions (uniform and log-normal) accounting for emissions and sensitivity uncertainties only. Third row (Log + CO_2): same as row 2, but also accounting for carbon cycle uncertainties. Bottom three rows (Log + all): same as row 3, but also accounting for ocean mixing and aerosol forcing uncertainties.

Case	Year	Percentile						
		1%	5%	25%	50%	75%	95%	99%
Uniform	2100	1.40	1.74	2.53	3.18	3.92	4.95	5.43
Log-normal	2100	1.37	1.71	2.40	3.00	3.69	4.71	5.26
Log + CO_2	2100	1.34	1.71	2.44	3.07	3.78	4.84	5.52
Log + all	2100	1.29	1.68	2.42	3.06	3.78	4.87	5.61
Log + all	2070	1.03	1.29	1.77	2.17	2.62	3.34	3.82
Log + all	2030	0.36	0.48	0.66	0.80	0.95	1.17	1.31

presented here place the warming range given in the TAR into a more realistic context by expressing the range in probabilistic form, accounting for emissions, climate sensitivity, carbon cycle, aerosol forcing, and ocean-mixing uncertainties. Our analysis is similar in principle to that of Titus and Narayanan [see figure 12 in (*31*)] in their assessment of future uncertainties in sea-level rise under the IS92 emissions scenarios, but we use more recent emissions scenarios and consider a wider range of input uncertainty factors.

Our results are only as realistic as the assumptions upon which they are based: that the SRES emissions scenarios are a realistic reflection of the range of emissions possibilities under a no-climate-policy assumption (*32*); that the TAR estimates of atmospheric composition and radiative forcing changes under these scenarios (*9*–*11*) (used here as our median values) are accurate; and that the AOGCMs used in the TAR as a basis for calibrating our simpler climate model (*4*) give realistic temperature responses. We have noted also that our analysis does not consider model structure uncertainties (beyond those that are captured by changing model parameter values), nor possible climate "surprises," both of which may lead to wider uncertainty ranges.

The assumption that the SRES scenarios are all equally likely warrants further investigation. Forcing for the higher emissions scenarios may be reduced if better account were taken of policies introduced in response to environmental changes other than climate. The SRES scenarios consider such policies comprehensively for SO_2 emissions projections, but not for tropospheric ozone precursors. Some of the high-emissions scenarios imply very high future tropospheric ozone levels (*11*), so accounting for responses to ozone-related pollution could reduce future radiative forcing in these cases by up to 1 W/m^2 by 2100.

An additional factor that might lead to lower emissions and radiative forcing at the high end of the SRES range is the possible effect of climate change on our ability to sustain the levels of economic growth assumed in these scenarios (*33*). Although climate feedbacks of this type are included in a number of integrated assessment models (*34*–*36*), their effect on the global economy for the high warming rates that are suggested here is unknown.

In summary, we have shown that the very high upper-limit warming rate of about 0.5°C/decade given in the IPCC TAR (*4*) is much less likely than warmings in the center of the distribution, which are about 0.3°C/decade. Even warming at this rate, however, is very large compared with the observed warming over the past century, and considerably larger than the rate of warming suggested in the IPCC SAR (*8*). In many of the scenarios considered, the rate of warming is still high at the end of the 21st century; further warming through the 22nd century would be virtually certain in these cases. Whether or not such rapid warming will occur and be sustained depends, of course, on actions taken to control climate change. If the near future were to follow a rapid warming pathway, and the expected impacts were to occur, it is likely that mitigation efforts would be initiated rapidly in the hope of reducing the rate and magnitude of change. Inertia in the climate system would, however, lead to only a slow response to such efforts and guarantee that future warming would still be large (*37*).

References and Notes

1. J. T. Houghton *et al.*, Eds., *Climate Change 2001: The Scientific Basis* (Cambridge Univ. Press, Cambridge, 2001).
2. N. Nakićenović, R. Swart, Eds., *Special Report on Emissions Scenarios* (Cambridge Univ. Press, Cambridge, 2000).
3. S. H. Schneider, *Nature* **411**, 17 (2001).
4. U. Cubasch, G. Meehl, in *Climate Change 2001: The Scientific Basis*, J. T. Houghton *et al.*, Eds. (Cambridge Univ. Press, Cambridge, 2001), pp. 525–582.
5. T. M. L. Wigley, S. C. B. Raper, *Nature* **357**, 293 (1992).
6. S. C. B. Raper, T. M. L. Wigley, R. A. Warrick, in *Sea-Level Rise and Coastal Subsidence: Causes, Consequences and Strategies*, J. Milliman, B. U. Haq, Eds. (Kluwer, Dordrecht, Netherlands, 1996), pp. 11–45.
7. S. C. B. Raper, J. M. Gregory, T. J. Osborn, *Clim. Dyn.* **17**, 601 (2001).
8. A. Kattenberg *et al.*, in *Climate Change 1995: The Science of Climate Change*, J. T. Houghton *et al.*, Eds. (Cambridge Univ. Press, Cambridge, 1996), pp. 285–357.
9. I. C. Prentice, in *Climate Change 2001: The Scientific Basis*, J. T. Houghton *et al.*, Eds. (Cambridge Univ. Press, Cambridge, 2001), pp. 183–237.
10. V. Ramaswamy, in *Climate Change 2001: The Scientific Basis*, J. T. Houghton *et al.*, Eds. (Cambridge Univ. Press, Cambridge, 2001), pp. 349–416.
11. D. Ehhalt, M. Prather, in *Climate Change 2001: The Scientific Basis*, J. T. Houghton *et al.*, Eds. (Cambridge Univ. Press, Cambridge, 2001), pp. 239–287.
12. In the SAR an earlier version of the same simple climate model was used, but with no direct calibration against AOGCMs.
13. R. N. Jones, *Clim. Change* **45**, 403 (2000).
14. R. H. Moss, S. H. Schneider, in *Guidance Papers on the Cross Cutting Issues of the Third Assessment Report of the IPCC*, R. Pachauri, T. Taniguchi, K. Tanaka, Eds. (World Meteorological Organization, Geneva, 2000), pp. 33–51.
15. As a consequence of the central limit theorem (CLT) in statistics, central values of the TAR range of warming should be more likely than the extremes because of the concatenation of a number of different input factors [see (*3*, *13*)]. If only the ranges of possible values for each input parameter were known, with each value within a given range equally likely, the CLT requires that, if the inputs combine additively, the output distribution will tend toward a Gaussian distribution (or bell curve).
16. T. M. L. Wigley, S .C. B. Raper, in *Climate and Sea Level Change: Observations, Projections and Implications*, R. A. Warrick, E. M. Barrow, T. M. L. Wigley, Eds. (Cambridge Univ. Press, Cambridge, 1993), pp. 111–133.
17. T. M. L. Wigley, in *Climate Change and the Agenda for Research*, T. Hanisch, Ed. (Westview, Boulder, CO, 1994), pp. 169–191.
18. T. M. L. Wigley, in *Climate Change and the Agenda for Research*, T. Hanisch, Ed. (Westview, Boulder, CO, 1994), pp. 193–222.
19. H. Visser, R. J. M. Folkert, J. Hoekstra, J. J. DeWolff, *Clim. Change* **45**, 421 (2000).
20. S. J. Smith, T. M. L. Wigley, N. Nakićenović, S. C. B. Raper, *Technol. Forecast. Soc. Change* **65**, 195 (2000).
21. T. M. L Wigley, S. J Smith, in *Do We Understand Climate Change?* (Norwegian Academy of Technological Sciences, Trondheim, 1998), pp. 185–195.
22. Although there are small thermal inertia effects arising from pre-1990 forcing differences, the primary driver for post-1990 temperature changes due to sulfate aerosol forcing is differences in SO_2 emissions relative to 1990.
23. The expert judgment survey of best-estimate sensitivities and their uncertainty (*38*), ignoring three outliers, gives a mean value of 2.8°C with a mean standard deviation of 1.5°C. A much larger uncertainty range is given in an assessment based solely on fitting model results to observed 1856 to 1997 temperature changes (*27*). Since the survey of (*38*) was carried out, confidence in the reality and magnitude of anthropogenic influences on climate has increased through pattern-based detection studies and paleoclimate analyses (*39*). Our sensitivity p.d.f. attempts to account for these diverse sources of information.
24. T. M. L. Wigley, *Tellus* **45B**, 409 (1993).
25. A. K. Jain, H. S. Kheshgi, D. J. Wuebbles, *Tellus* **48B**, 583 (1996).
26. F. Joos, M. Bruno, R. Fink, U. Siegenthaler, T. F. Stocker, C. LeQuere, *Tellus* **48B**, 397 (1996).
27. N. Andronova, M. E. Schlesinger, *J. Geophys. Res.*, in press.
28. Because of climate feedbacks on the carbon cycle, these forcing estimates also depend on the temperature projections. Our median forcing estimates for each scenario differ slightly from those used in the TAR (*4*) because we have corrected an error in the formula for tropospheric ozone abundance given in (*11*) that was not noticed in time to be used in the TAR temperature calculations. Correcting for this error reduces high-end TAR temperature projections by up to 0.2°C in 2100.
29. M. G. Morgan, M. Henrion, *Uncertainty* (Cambridge Univ. Press, Cambridge, 1990).
30. T. M. L. Wigley, *Geophys. Res. Lett.* **27**, 4101 (2000).
31. J. G. Titus, V. Narayanan, *Clim. Change* **33**, 151 (1996).
32. Note that SRES scenarios were not designed to span the full range of possibilities.
33. It should be noted that the relationship between economic growth and emissions is not a simple one, and reduced economic growth need not necessarily lead to reduced emissions.
34. H. Dowlatabadi, M. G. Morgan, *Energy Policy* **21**, 209 (1993).
35. R. S. J. Tol, *Special Issue on the Costs of the Kyoto Protocol*, *Energy J.* 130–156 (1999).
36. A. S. Manne, R. Mendelsohn, R. Richels, *Energy Policy* **23**, 17 (1993).
37. T. M. L. Wigley, R. Richels, J. A. Edmonds, *Nature* **379**, 240 (1996).
38. M. G. Morgan, D. W. Keith, *Environ. Sci. Technol.* **29**, 468A (1995).
39. J. F. B. Mitchell, D. J. Karoly, in *Climate Change 2001: The Scientific Basis*, J. T. Houghton *et al.*, Eds. (Cambridge Univ. Press, Cambridge, 2001), pp. 695–738.
40. M. R. Allen *et al.*, *Nature* **407**, 617 (2000).

41. Supported by the U.K. Department of the Environment, Transport and the Regions, HGF Strategiefonds Projekt 2000/13, and ACACIA, a joint activity of EPRI and the National Center for Atmospheric Research (NCAR). NCAR is sponsored by the U.S. National Science Foundation. Comments from S. J. Smith, B. D. Santer, and two referees helped improve the paper.

13 April 2001; accepted 21 June 2001